EMTENSOR ASSIGNMENT

-Submitted by,
Sarrvesh N

OBJECTIVE :

Design, train, and validate an open-source AI model to accurately segment anatomical regions of the brain (e.g., gray matter, white matter, ventricles, hippocampus) and identify abnormalities (e.g., tumors, lesions, atrophy) in 3D neuroimaging data (e.g., MRI, CT). The framework must incorporate statistical analysis to quantify uncertainty, validate model performance, and correlate findings with clinical outcomes for improved diagnostic decision-making.

PROPOSED WORK SYNOPSIS :

- Designed, trained and validated UNet model for Brain Tumor detection and segmentation.
- Incorporated statistical analysis to validate model performance on segmenting brain tumor.
- Brain anatomy segmentation is carried out using FastSurfer open-source framework.

DETAILED METHODOLOGY :

> **DATASET USED :**
- BRATS dataset
- No:of training samples : 185
- No:of testing samples : 147
- Each training sample contains 5 different .nii or NIfTI files.
  - **T1 Weighted file**, which highlights anatomical details and is suitable for anatomical segmentation.
  - **T1ce file**, which is same as T1 but with contrast enhanced features, where tumor also kind of appears bright.
  - **FLAIR file,** which highlights edema (tumor) and is suitable for brain edema segmentation tasks.
  - **T2 file,** which highlights cerebrospinal fluids (CSF) and edema.
  - **Segmentation file,** the label/segmentation mask/ground truth which actually has the segmented tumor region alone. This is used for training the UNet model for tumor segmentation.

➢ **MODELS USED :**

3D UNet :

This model is an 3D U-Net designed for medical image segmentation. Brain tumor segmentation task is carried out using this model. It incorporates attention gates, residual connections, and dropout regularization to improve feature extraction and segmentation accuracy.

- **KEY FEATURES :**
  - **Attention Blocks:** Improves feature selection by emphasizing relevant regions.
  - **Residual Blocks:** Enables deeper feature learning while mitigating vanishing gradient issues.
  - **3D Convolutions:** Captures spatial context across slices for better segmentation.
  - **Dropout & Batch Normalization:** Enhances model generalization and stability.

- **ARCHITECTURE :**
  - **Encoder :**
    1. Four levels of convolutional blocks with residual connections.
    2. Max pooling layers for down sampling
  - **Bottleneck :**
    1. Deepest convolutional block for high level feature extraction.
  - **Decoder :**
    1. Transposed convolutions for up sampling.
    2. Attention gates to refine skip connections.
    3. Merges encoder features for better localization.
  - **Output layer :**
    1. 3D softmax activation for multi-class segmentation.

FAST-SURFER :

FastSurfer is an opensource, deep-learning-based alternative to FreeSurfer. It takes a T1-weighted MRI scan (.nii or .nii.gz) as input and automatically processes it to generate brain region segmentations with labelled structures. This framework is openly available in GitHub. If FastSurfer is not available locally, it clones the repository and sets up the execution environment. After execution, the class verifies output consistency, resamples data if needed, and provides a FastSurfer brain region mapping for easy interpretation. This process fully automates MRI segmentation, ensuring efficiency and accuracy.

- **IMPLEMENTED KEY FUNCTIONALITIES**
  - **Input Handling & Setup :**
    1. Validates the MRI file path.
    2. Sets up necessary directories for segmentation output.
    3. Clones FastSurfer from GitHub if not already present.
  - **Dependency Management :**
    1. Checks and installs required Python packages like nibabel, scikit-image, torch, and matplotlib.
  - **FastSurfer Segmentation Execution :**
    1. Runs the script with optimized parameters.
    2. Ensures the script is executable before execution.
    3. Handles segmentation failures with error messages.
  - **Segmentation Verification :**
    1. Checks for output files (aseg.mgz, aparc.DKTatlas+aseg.deep.mgz).
    2. Loads and compares segmentation with original MRI dimensions.
    3. Resamples segmentation data if dimensions mismatch.
  - **Brain Region Mapping :**
    1. Provides a dictionary of FreeSurfer brain region labels with their corresponding IDs and legend colours (e.g., Left Hippocampus, Right Thalamus, White matter, Gray matter etc,.).

➤ STATISTICAL ANALYSIS AND PERFORMANCE METRICS :

PERFORMANCE METRICS :

1. **Dice Coefficient (Dice Score) :** Measures segmentation accuracy by comparing model predictions with ground truth.

$$Dice \ = \ \frac{2TP}{2TP + FP + FN}$$

2. **Sensitivity (Recall) :** Measures how well the model identifies actual positives (tumor regions).
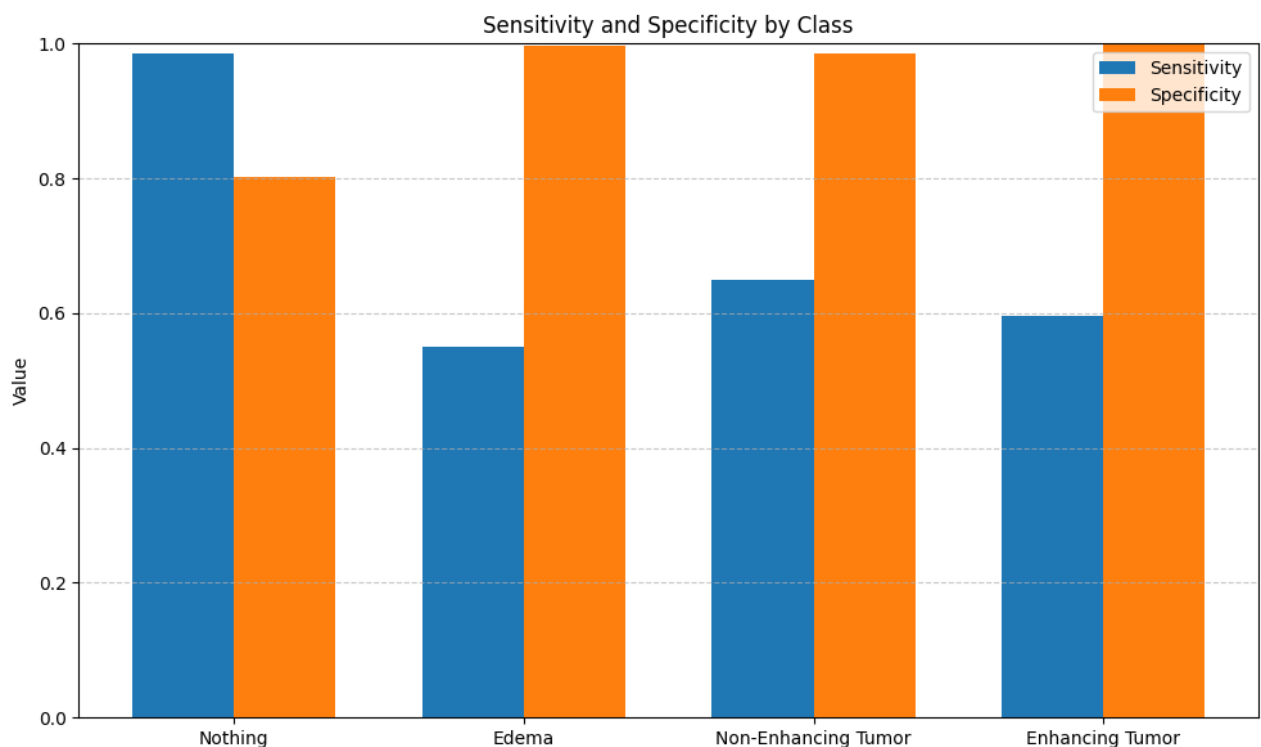
$$Sensitivity \ = \ \frac{TP}{TP + FN}$$

3. **Specificity :** Measures how well the model avoids false positives (correctly identifying non-tumor regions).
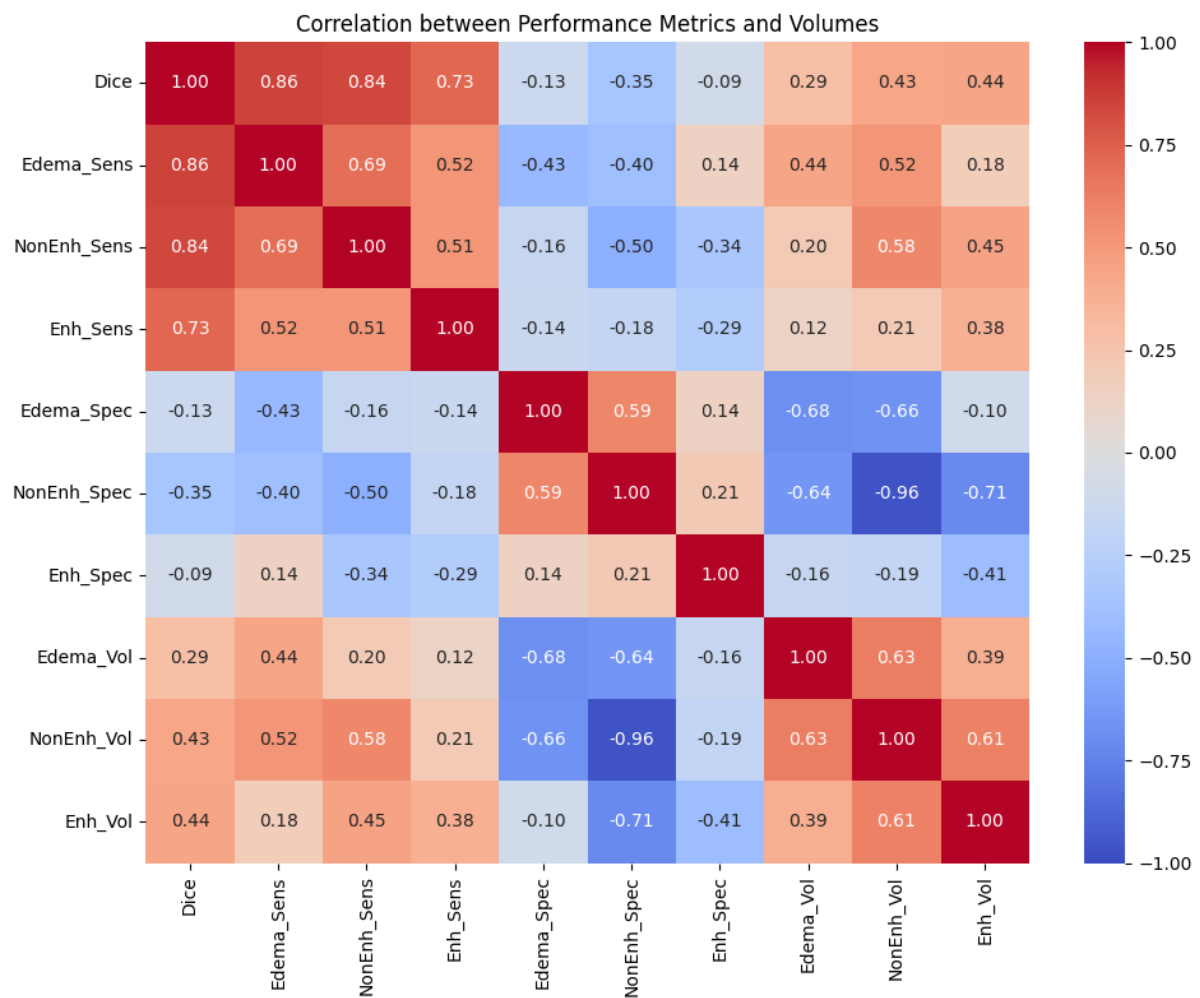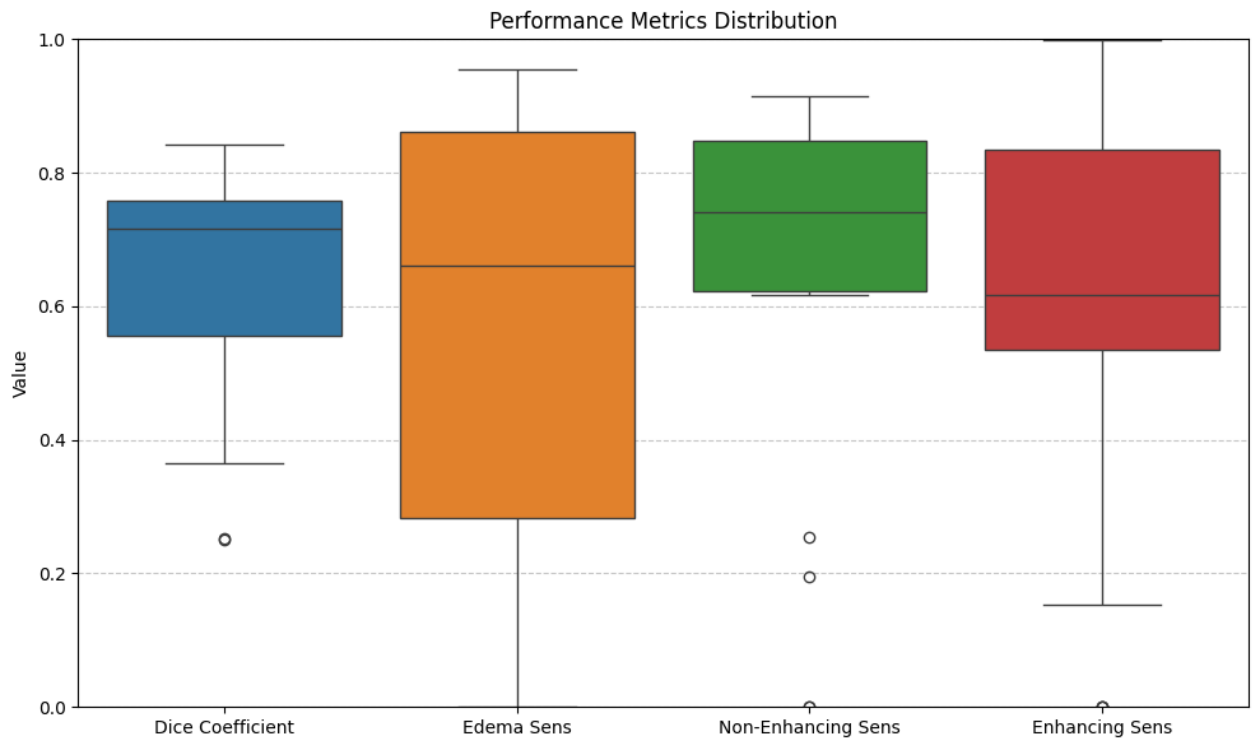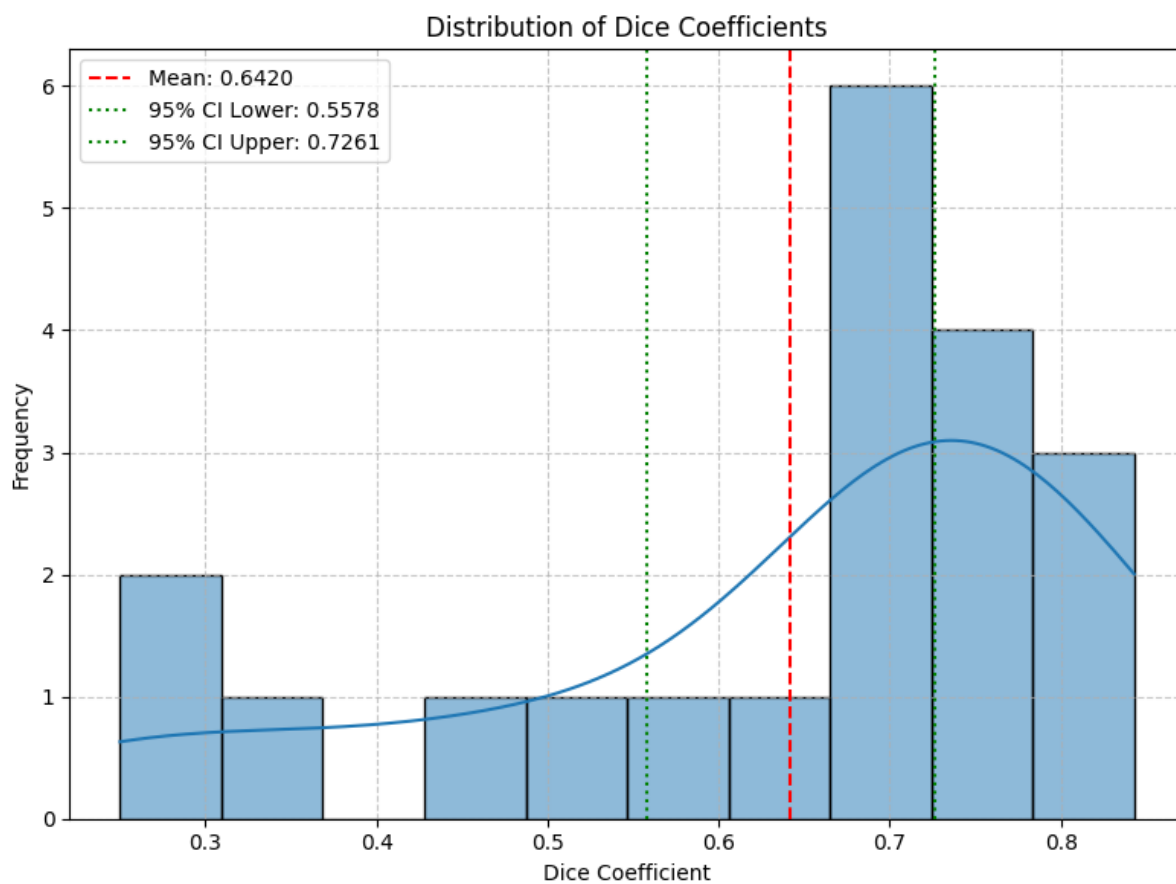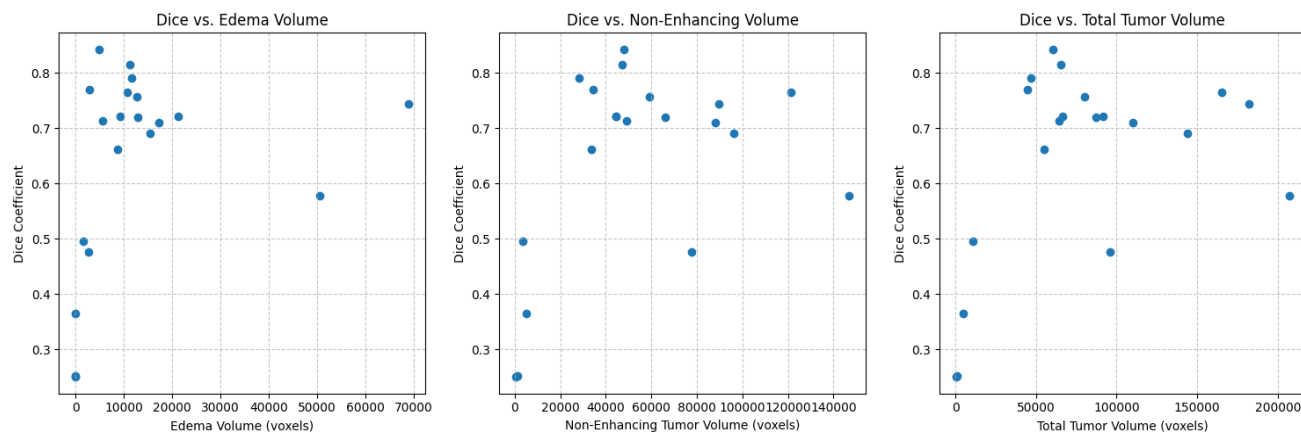
$$Specifity \ = \ \frac{TN}{TN + FP}$$

STATISTICAL ANALYSIS :

1. **Mean and Standard Deviation (SD) :** Provides an average and spread of Dice coefficient, sensitivity, specificity, and volume.
2. **Standard Error (SE) :** Measures the precision of the mean estimate.
3. **95% Confidence Interval (CI) :** Uses the t-distribution to estimate the range within which the true mean likely falls.
4. **ANOVA (Analysis of Variance) :** Tests if there is a significant difference in sensitivity across different tumor classes.
5. **Heatmap Visualization :** Displays correlation strengths and directions between variables.
6. **Volume-Based Analysis :** Computes average segmented volume per class to compare model predictions with real anatomical structures.

VISUALIZATIONS :

Performance Metrics Distribution

Correlation between Performance Metrics and Volumes

Dice vs. Edema Volume

Dice vs. Non-Enhancing Volume

Dice vs. Total Tumor Volume

Distribution of Dice Coefficients

Mean: 0.6420
95% CI Lower: 0.5578
95% CI Upper: 0.7261

STATISTICAL AND PERFORMANCE RESULTS :

```
Mean Dice Loss 0.3580439567565918
Mean Dice Coefficient(Accuracy) 0.6419560447335243

Mean Sensitivity for class 0 0.9860865830599777
Mean Specificity for class 0 0.8025275421030214

Mean Sensitivity for class 1 0.5504838861600057
Mean Specificity for class 1 0.9966057532017143

Mean Sensitivity for class 2 0.6492498974696218
Mean Specificity for class 2 0.9856655131897238

Mean Sensitivity for class 3 0.5955052888269023
Mean Specificity for class 3 0.9983529088954486
```

```
===== STATISTICAL ANALYSIS =====

Descriptive Statistics with 95% Confidence Intervals:
Dice Coefficient: 0.6420 ± 0.1752 (95% CI: 0.5578 to 0.7261)

Nothing:
  Sensitivity: 0.9861 ± 0.0116 (95% CI: 0.9805 to 0.9916)
  Specificity: 0.8025 ± 0.3129 (95% CI: 0.6523 to 0.9528)
  Average Volume: 2017982.4 ± 57547.6 voxels

Edema:
  Sensitivity: 0.5505 ± 0.3494 (95% CI: 0.3827 to 0.7183)
  Specificity: 0.9966 ± 0.0048 (95% CI: 0.9943 to 0.9989)
  Average Volume: 13394.4 ± 16799.0 voxels

Non-Enhancing Tumor:
  Sensitivity: 0.6492 ± 0.2882 (95% CI: 0.5109 to 0.7876)
  Specificity: 0.9857 ± 0.0121 (95% CI: 0.9799 to 0.9915)
  Average Volume: 54221.1 ± 39048.9 voxels

Enhancing Tumor:
  Sensitivity: 0.5955 ± 0.3185 (95% CI: 0.4426 to 0.7484)
  Specificity: 0.9984 ± 0.0016 (95% CI: 0.9976 to 0.9991)
  Average Volume: 11554.0 ± 9584.6 voxels

Hypothesis Testing - Sensitivity Across Tumor Classes:
ANOVA: F=0.4546, p-value=0.6370
No significant difference in sensitivity between tumor classes (p>=0.05)
```
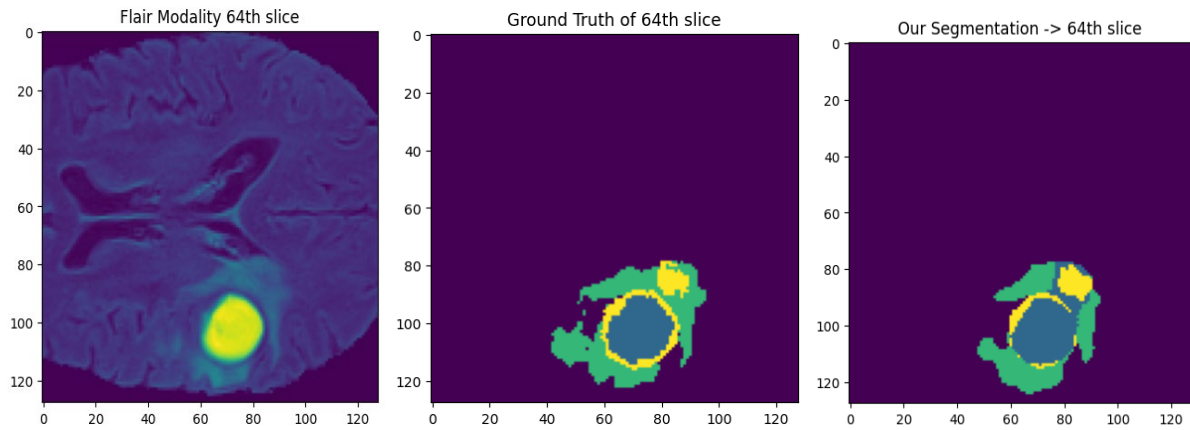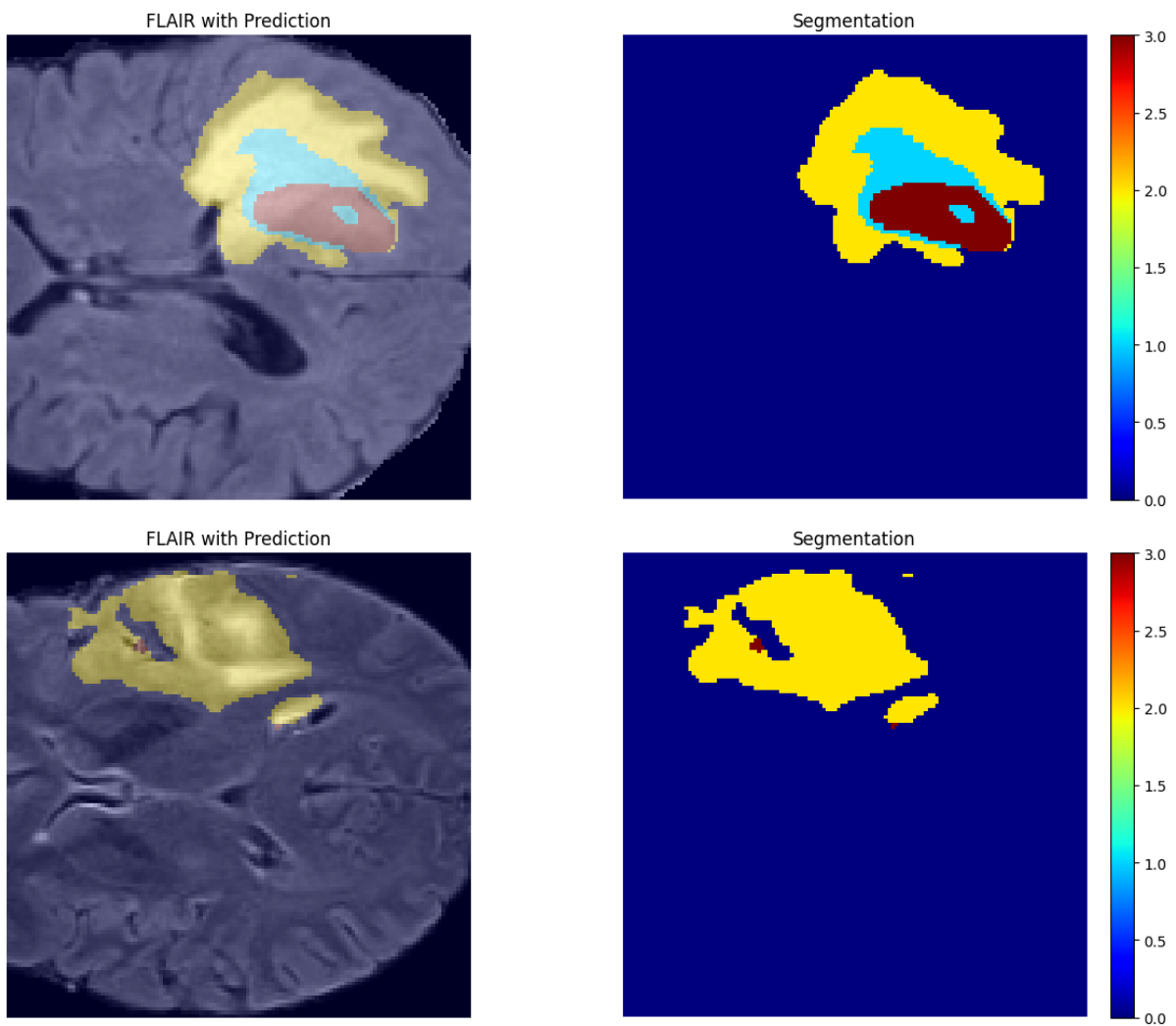
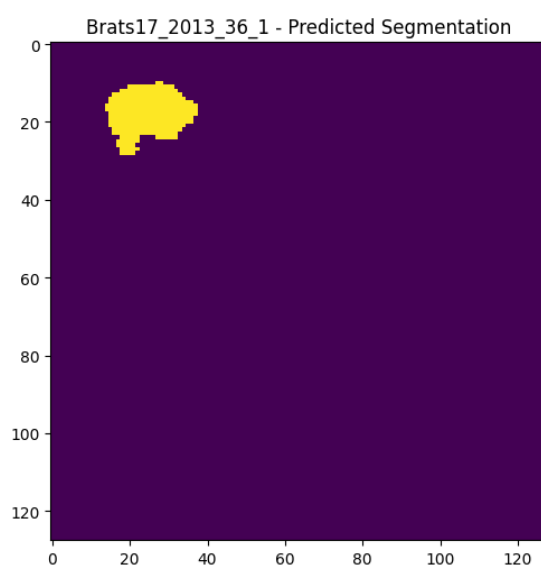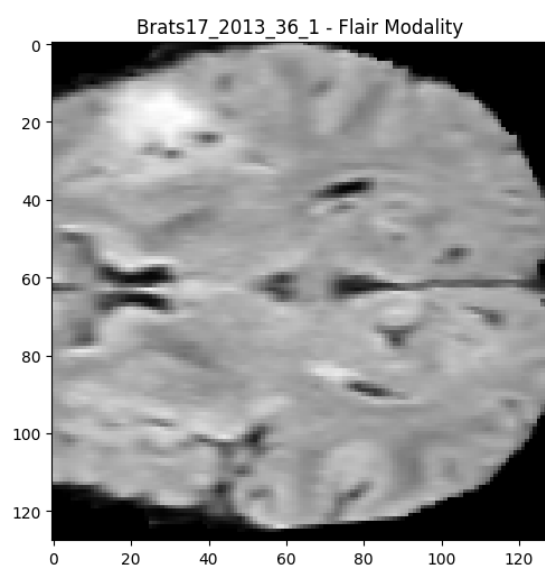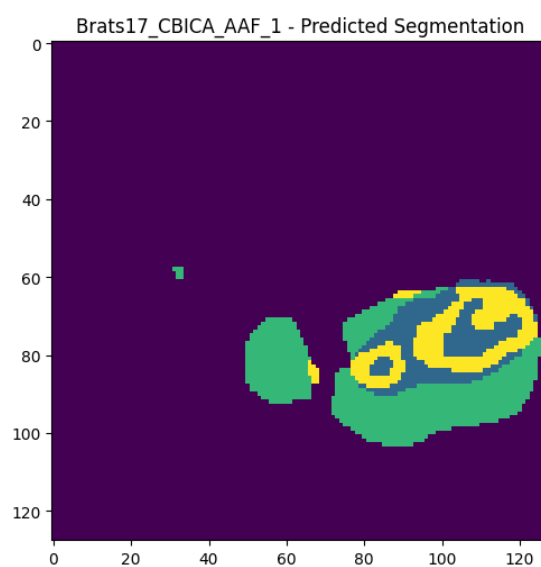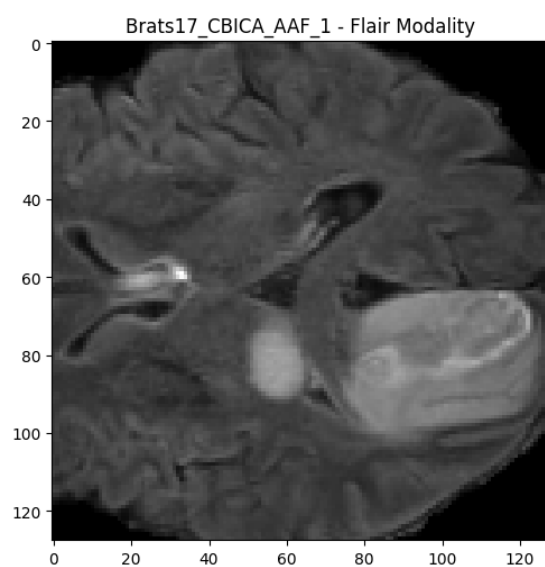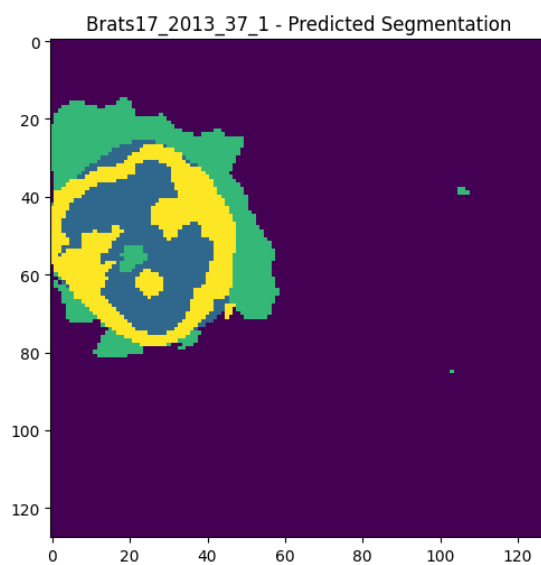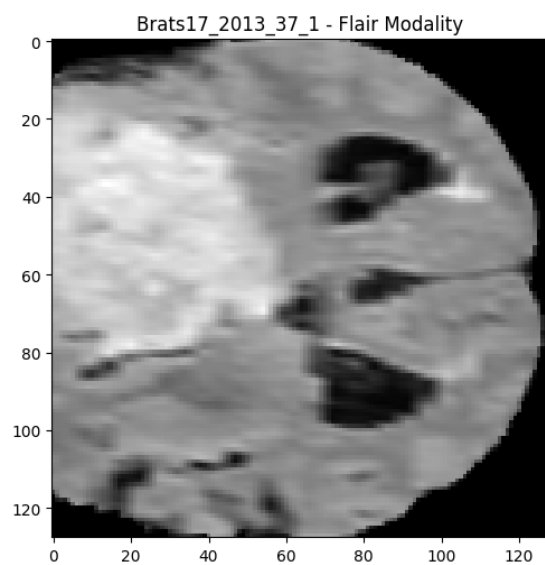# OUTPUT RESULTS AND INFERENCE :

TUMOR SEGMENTATION - With Ground Truth

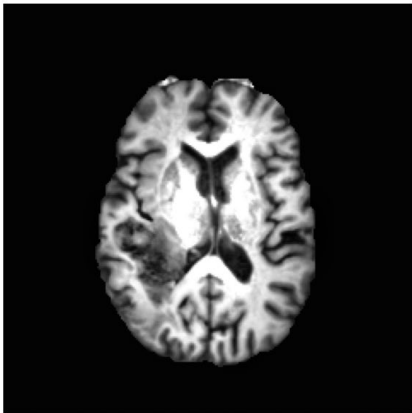## TUMOR SEGMENTATION - Without Ground Truth

Brats17_2013_37_1 - Flair Modality **Brats17_2013_37_1 - Predicted Segmentation**

Brats17_CBICA_AAF_1 - Flair Modality **Brats17_CBICA_AAF_1 - Predicted Segmentation**

Brats17_2013_36_1 - Flair Modality **Brats17_2013_36_1 - Predicted Segmentation**
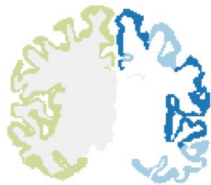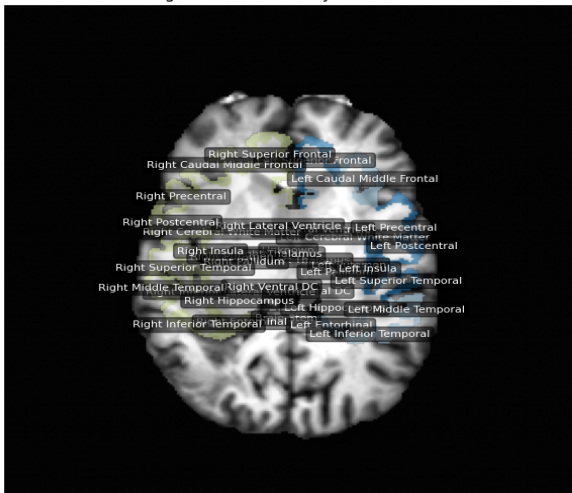
ANATOMY SEGMENTATION - Axial View

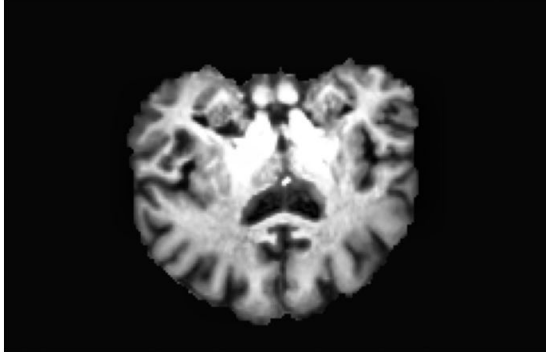Original T1 Image (axial view)
Slice: 77

Segmentation Mask

Segmentation Overlay with Labels

- 0: Unknown
- 2: Left Cerebral White Matter
- 4: Left Lateral Ventricle
- 5: Left Inferior Lateral Ventricle
- 10: Left Thalamus
- 11: Left Caudate
- 12: Left Putamen
- 13: Left Pallidum
- 14: 3rd Ventricle
- 16: Brain Stem
- 17: Left Hippocampus
- 18: Left Amygdala
- 24: CSF
- 28: Left Ventral DC
- 41: Right Cerebral White Matter
- 43: Right Lateral Ventricle
- 44: Right Inferior Lateral Ventricle
- 49: Right Thalamus
- 50: Right Caudate
- 51: Right Putamen
- 52: Right Pallidum
- 53: Right Hippocampus
- 54: Right Amygdala
- 60: Right Ventral DC
- 63: Right Choroid Plexus
- 1002: Left Caudal Anterior Cingulate
- 1003: Left Caudal Middle Frontal
- 1006: Left Entorhinal
- 1007: Left Fusiform
- 1009: Left Inferior Temporal
- 1015: Left Middle Temporal
- 1022: Left Postcentral
- 1023: Left Posterior Cingulate
- 1024: Left Precentral
- 1028: Left Superior Frontal
- 1030: Left Superior Temporal
- 1035: Left Insula
- 2003: Right Caudal Middle Frontal
- 2006: Right Entorhinal
- 2007: Right Fusiform
- 2009: Right Inferior Temporal
- 2015: Right Middle Temporal
- 2016: Right Parahippocampal
- 2022: Right Postcentral
- 2023: Right Posterior Cingulate
- 2024: Right Precentral
- 2028: Right Superior Frontal
- 2030: Right Superior Temporal
- 2034: Right Transverse Temporal
- 2035: Right Insula
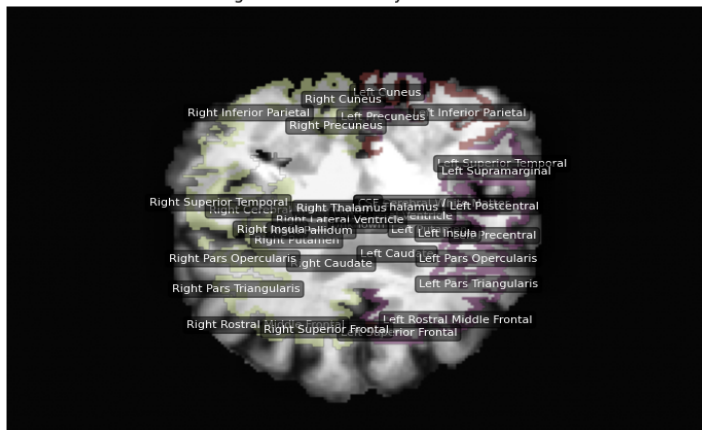
ANATOMY SEGMENTATION - Coronal View

Original T1 Image (coronal view)
Slice: 120

Segmentation Mask

Segmentation Overlay with Labels

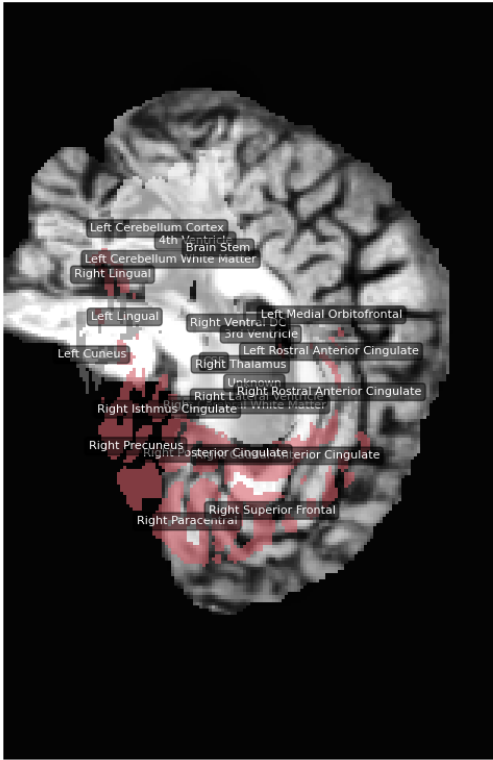| Label	Region
0:	Unknown
2:	Left Cerebral White Matter
4:	Left Lateral Ventricle
10:	Left Thalamus
11:	Left Caudate
12:	Left Putamen
24:	CSF
31:	Left Choroid Plexus
41:	Right Cerebral White Matter
43:	Right Lateral Ventricle
49:	Right Thalamus
50:	Right Caudate
51:	Right Putamen
52:	Right Pallidum
53:	Right Hippocampus
63:	Right Choroid Plexus
1005:	Left Cuneus
1008:	Left Inferior Parietal
1010:	Left Isthmus Cingulate
1014:	Left Medial Orbitofrontal
1018:	Left Pars Opercularis
1020:	Left Pars Triangularis
1022:	Left Postcentral
1024:	Left Precentral
1025:	Left Precuneus
1026:	Left Rostral Anterior Cingulate
1027:	Left Rostral Middle Frontal
1028:	Left Superior Frontal
1029:	Left Superior Parietal
1030:	Left Superior Temporal
1031:	Left Supramarginal
1035:	Left Insula
2005:	Right Cuneus
2008:	Right Inferior Parietal
2010:	Right Isthmus Cingulate
2011:	Right Lateral Occipital
2012:	Right Lateral Orbitofrontal
2014:	Right Medial Orbitofrontal
2015:	Right Middle Temporal
2018:	Right Pars Opercularis
2019:	Right Pars Orbitalis
2020:	Right Pars Triangularis
2022:	Right Postcentral
2024:	Right Precentral
2025:	Right Precuneus
2026:	Right Rostral Anterior Cingulate
2027:	Right Rostral Middle Frontal
2028:	Right Superior Frontal
2029:	Right Superior Parietal
2030:	Right Superior Temporal
2034:	Right Transverse Temporal
2035:	Right Insula

ANATOMY SEGMENTATION - Sagittal View

Original T1 Image (sagittal view)
Slice: 120

Segmentation Mask

Segmentation Overlay with Labels

Left Cerebellum Cortex
4th Ventricle
Brain Stem
Left Cerebellum White Matter
Right Lingual
Left Medial Orbitofrontal
Left Lingual
Right Ventral DC
3rd Ventricle
Left Rostral Anterior Cingulate
Left Cuneus
Right Thalamus
Unknown
Right Rostral Anterior Cingulate
Right Isthmus Cingulate
Right Precuneus
Right Posterior Cingulate
Right Superior Frontal
Right Paracentral

- 0: Unknown
- 2: Left Cerebral White Matter
- 7: Left Cerebellum White Matter
- 8: Left Cerebellum Cortex
- 14: 3rd Ventricle
- 15: 4th Ventricle
- 16: Brain Stem
- 24: CSF
- 41: Right Cerebral White Matter
- 43: Right Lateral Ventricle
- 46: Right Cerebellum White Matter
- 47: Right Cerebellum Cortex
- 49: Right Thalamus
- 60: Right Ventral DC
- 63: Right Choroid Plexus
- 1005: Left Cuneus
- 1010: Left Isthmus Cingulate
- 1013: Left Lingual
- 1014: Left Medial Orbitofrontal
- 1026: Left Rostral Anterior Cingulate
- 1028: Left Superior Frontal
- 2002: Right Caudal Anterior Cingulate
- 2005: Right Cuneus
- 2010: Right Isthmus Cingulate
- 2013: Right Lingual
- 2014: Right Medial Orbitofrontal
- 2017: Right Paracentral
- 2022: Right Postcentral
- 2023: Right Posterior Cingulate
- 2025: Right Precuneus
- 2026: Right Rostral Anterior Cingulate
- 2028: Right Superior Frontal
- 2029: Right Superior Parietal

INFERENCE :

The 3D Unet model demonstrates promising performance in brain tumor segmentation across multiple tissue classes. The overall Dice coefficient of 0.6420 (95% CI: 0.5578 to 0.7261) indicates moderate segmentation accuracy. With respect to the class-specific metrics, the model excels in identifying normal tissue (Class 0) with exceptional sensitivity (0.9861) but moderate specificity (0.8025). For pathological tissues, the model shows balanced performance for non-enhancing tumors (Class 2) with sensitivity of 0.6492 and high specificity of 0.9857. The model achieves the highest specificity for enhancing tumors (Class 3) at 0.9984, though with moderate sensitivity (0.5955). Edema (Class 1) shows similar performance patterns with high specificity (0.9966) but lower sensitivity (0.5505).

The ANOVA results (p=0.6370) indicate no statistically significant differences in sensitivity across tumor classes, suggesting consistent detection capability regardless of tumor type.

The FastSurfer anatomical segmentation complements these findings by providing detailed brain region labeling, which could help identify different parts/regions of the brain through a given T1-weighted MRI file ie, a NIfTI file. This may also help in contextualizing tumor locations relative to critical brain structures, potentially enhancing clinical interpretability of the segmentation results.